

1 **Original Article**

2

3 **Early Reduction of SARS-CoV-2 Replication in Bronchial Epithelium by**

4 **Kinin B₂ Receptor Antagonism**

5 **Short title:** B₂R Antagonist Suppresses SARS-CoV-2 Replication

6

7 Constanze A. Jakwerth^{1*}, Martin Feuerherd^{2*}, Ferdinand M. Guerth¹, Madlen Oelsner¹, Linda

8 Schellhammer³, Johanna Giglberger^{1,6}, Lisa Pechtold⁶, Claudia Jerin^{1,6}, Luisa Kugler⁶, Carolin

9 Mogler⁴, Bernhard Haller⁵, Anna Erb¹, Barbara Wollenberg⁶, Christoph D. Spinner⁷, Thorsten

10 Buch³, Ulrike Protzer², Carsten B. Schmidt-Weber^{1,§}, Ulrich M. Zissler^{1,#}, Adam M. Chaker^{1,6#}

11

12 1) Center of Allergy & Environment (ZAUM), Technical University of Munich and Helmholtz
13 Center Munich, German Research Center for Environmental Health, Member of the German
14 Center for Lung Research (DZL), CPC-M, Munich, Germany

15 2) Institute of Virology, Technical University of Munich/Helmholtz Zentrum München,
16 Munich, Germany; German Center of Infectiology Research (DZIF), Munich partner site,
17 Munich, Germany

18 3) Institute of Laboratory Animal Science, University of Zurich, Zurich, Switzerland

19 4) Institute of Pathology, Technical University Munich, Munich, Germany

20 5) Institute of Medical Informatics, Statistics and Epidemiology, Medical School, Technical
21 University of Munich

22 6) Department of Otorhinolaryngology and Head and Neck Surgery, Medical School, Technical
23 University of Munich, Germany

24 7) Department of Internal Medicine II, University Hospital rechts der Isar, Medical School,
25 Technical University of Munich, Munich, Germany

26 *) These authors contributed equally

27 #) These senior authors contributed equally

28

29 §) Corresponding author:

30 Prof. Dr. Carsten B. Schmidt-Weber, Chair & Director

31 Center of Allergy & Environment (ZAUM)

32 Technical University and Helmholtz Center Munich

33 Biedersteiner Str. 29

34 80202 Munich, Germany

35 Email: csweber@tum.de

36 **NOTE:** This preprint reports new research that has not been certified by peer review and should not be used to guide clinical practice.

37

38 **Conflict of interests:**

39 Dr. Jakwerth reports grants from Federal Ministry of Education and Research, grants from
40 European Institute of Innovation & Technology (EIT), during the conduct of the study. Mr.
41 Feuerherd reports personal fees from Helmholtz Zentrum München and Dr. Höhnle AG, outside
42 the submitted work. Dr. Spinner reports grants, personal fees, non-financial support and other
43 from AbbVie, grants, personal fees, non-financial support and other from Apeiron, personal
44 fees from Formycon, grants, personal fees, non-financial support and other from Gilead
45 Sciences, grants, personal fees and other from Eli Lilly, grants, personal fees, non-financial
46 support and other from Janssen-Cilag, grants, personal fees, non-financial support and other
47 from GSK/ViiV Healthcare, grants, personal fees, non-financial support and other from MSD,
48 outside the submitted work. Prof. Dr. Buch reports personal fees from Virometix AG, other
49 from Virometix AG, other from Trials24 GmbH, other from Clemedi AG, outside the submitted
50 work. Prof. Dr. Protzer reports grants from the Federal Ministry of Education and Research, the
51 German Center for Infection Research (DZIF), the German Research Foundation (DFG), the
52 European Union via Horizon 2020 and the Bavarian Research Foundation during conduct of
53 the study. She receives personal fees as an ad hoc scientific advisor from Abbvie, Arbutus,
54 Gilead, GSK, Johnson & Johnson, Vaccitech. Prof. Dr. Schmidt-Weber reports grants from
55 German Center for Lung Research (DZL), grants from Comprehensive Pulmonary Lung Center
56 (CPC) Munich during the conduct of the study. Personal Fees from Allergopharma and
57 Bencard, outside the submitted work. Dr. Zissler reports grants from Federal Ministry of
58 Education and Research, during the conduct of the study. Dr. Chaker reports grants for clinical
59 studies and research and other from Allergopharma, ALK Abello, AstraZeneca, Bencard /
60 Allergen Therapeutics, ASIT Biotech, Lofarma, GSK, Novartis, LETI, Immunotek, Roche,
61 Sanofi Genzyme, Zeller and from the European Institute of Technology (EIT); has received
62 travel support from the European Academy of Allergy and Clinical Immunology (EAACI),
63 DGAKI, all outside the submitted work. In addition, Drs. Jakwerth, Feuerherd, Protzer,

64 Schmidt-Weber, Zissler and Chaker are named as inventors on the patent application 'Novel
65 approaches for treatment of SARS-CoV2-Infection in a patient'. Mr. Guerth, Ms. Oelsner, Dr.
66 Schellhammer, Ms. Giglberger, Ms. Pechtold, Dr. Jerin, Ms. Kugler, Dr. Mogler, Dr. Haller,
67 Ms. Erb, Prof. Dr. Wollenberg have nothing to disclose.

68

69 **Funding:** This study was supported by funding from the German Center of Lung Research
70 (DZL), the Comprehensive Pneumology Center (CPC) Munich, the German Research
71 Foundation (DFG; 398577603, TR22), and the Federal Ministry of Education and Research
72 (ESCAPE; 01KI20169A).

73

74 **Author contributions:**

75 Study design A.M.C., C.S.W., U.P., C.A.J., M.F., U.M.Z., T.B.; collection of patient samples
76 A.M.C., J.G., L.P., Cl.J., L.K.; conduction of experiment C.A.J., M.F., F.G., M.O., C.M., L.S.,
77 J.G., L.K.; data collection C.A.J., M.F., F.G., M.O., U.M.Z., C.M., L.S., J.G., L.P., Cl.J., L.K.;
78 data analysis C.A.J., M.F., F.G., A.E., U.M.Z., C.M., B.H., L.S.; data interpretation A.M.C.,
79 C.S.W., U.P., C.A.J., M.F., U.M.Z., C.M., B.H., C.D.S., B.W., L.S., T.B.; literature search
80 A.M.C., C.S.W., C.A.J., M.F., U.M.Z., A.E.; writing all authors.

81

82

83 **ABSTRACT (247/250 words)**

84 **Background:** SARS-CoV2 has evolved to enter the host via the ACE2 receptor which is part
85 of the Kinin-kallirein pathway. This complex pathway is only poorly understood in context of
86 immune regulation but critical to control infection. This study examines SARS-CoV2 infection
87 and epithelial mechanisms of the kinin-kallikrein system at the kinin B₂ receptor level in SARS-
88 CoV-2 infection that is of direct translational relevance.

89 **Methods:** From acute SARS-CoV-2-positive patients and -negative controls, transcriptomes of
90 nasal brushings were analyzed. Primary airway epithelial cells (NHBEs) were infected with
91 SARS-CoV-2 and treated with the approved B₂R antagonist icatibant. SARS-CoV-2 RNA RT-
92 qPCR, cytotoxicity assays, plaque assays and transcriptome analyses were performed. The
93 treatment effect was further studied in a murine airway inflammation model *in vivo*.

94 **Results:** Here, we report a broad and strong upregulation of kallikreins and the kinin B₂ receptor
95 (B₂R) in the nasal mucosa of acutely symptomatic SARS-CoV-2-positive patients. A B₂R
96 antagonist impeded SARS-CoV-2 replication and spread in NHBEs, as determined in plaque
97 assays on Vero E6 cells. B₂R antagonism reduced the expression of SARS-CoV-2 entry
98 receptor ACE2 *in vitro* and in a murine airway inflammation model *in vivo*. In addition, it
99 suppressed gene expression broadly, particularly genes involved in G-protein-coupled-receptor
100 signaling and ion transport.

101 **Conclusions:** In summary, this study provides evidence that treatment with B₂R antagonists
102 protects airway epithelial cells from SARS-CoV-2 by inhibiting its replication and spread,
103 through the reduction of ACE2 levels and the interference with several cellular signaling
104 processes. Future clinical studies need to shed light on the airway protection potential of
105 approved B₂R antagonists, like icatibant, in the treatment of early-stage COVID-19.

106

107 **Key words:** ACE2; COVID-19; kinin B₂R antagonist; kinin-kallikrein system; SARS-CoV-2

108

109 **Abbreviations:**

110	ACE2	angiotensin-converting enzyme 2
111	ant-B ₂ R	kinin B ₂ receptor antagonist
112	<i>BDKRB1</i>	kinin B ₁ receptor (gene name)
113	<i>BDKRB2</i>	kinin B ₂ receptor (gene name)
114	B ₁ R	kinin B ₁ receptor
115	B ₂ R	kinin B ₂ receptor
116	B ₂ R antagonist	kinin B ₂ receptor antagonist
117	CAS	contact activation system
118	COVID-19	coronavirus disease of 2019
119	DABK	des-Arg ⁹ -bradykinin
120	GPCR	G protein-coupled receptor
121	HC	hydrocortisone
122	HMW-kininogen	high-molecular-weight-kininogen
123	IC ₅₀	half maximal inhibitory concentration
124	KKS	kinin-kallikrein system
125	LDH	lactate dehydrogenase
126	NHBE	normal human bronchial epithelial cells
127	RAS	renin-angiotensin system
128	SARS-CoV-2	Severe Acute Respiratory Syndrome Coronavirus-2
129	TMPRSS	transmembrane serine protease

130

131 **Word count: 3,476 / 3,500**

132 **1 INTRODUCTION**

133 SARS-CoV-2 vaccines have been approved worldwide since the end of 2020 and are starting
134 to show their protective effects in public health.^{1,2} Even with vaccines at hand, an important
135 medical need for therapeutic approaches for COVID-19 remains: Parts of the population refrain
136 from vaccination or are not eligible for it, immunocompromised individuals may not mount a
137 sufficient immune response after vaccination and escape variants, such as the currently
138 spreading SARS-CoV-2 variant Delta³, may breach the protection afforded by the vaccines.⁴⁻⁹
139 Key factors for SARS-CoV-2 cell entry are two cell surface molecules, the angiotensin-
140 converting enzyme 2 (ACE2) and the transmembrane serine protease (TMPRSS2).¹⁰ TMPRSS2
141 cleaves the coronaviral spike protein and primes it for cell fusion, while ACE2 enables the virus
142 particle to enter the cell by binding of its spike protein.^{11,12} The latter acts as central component
143 in its function as terminal carboxypeptidase in the counter-regulatory axis of the renin-
144 angiotensin system (RAS) and the contact activation system (CAS),^{10,13} which initiates blood
145 coagulation and can additionally activate the kinin-kallikrein system (KKS).¹⁴ In its role in the
146 RAS, ACE2 has anti-vasoconstrictive and anti-inflammatory effects by hydrolyzing the
147 vasoconstrictive and tissue-damaging angiotensin II, which contributes to airway remodeling
148 and fibrosis,^{15,16} to angiotensin (1-7).¹⁷ In its role in the KKS, ACE2 further hydrolyzes
149 vasoactive peptides such as des-Arg9-bradykinin (DABK), which activates the inflammatory
150 axis of the KKS.^{18,19} While DABK is the ligand of the inducible kinin B₁ receptor (*BDKRB1*;
151 B₁ receptor),²⁰ bradykinin, the end product of the KKS cascade, binds to the constitutively
152 expressed kinin B₂ receptor (*BDKRB2*; B₂ receptor; B₂R) and activates it.²¹ Bradykinin
153 mediates its pro-inflammatory effects via the B₂ receptor, by eliciting a variety of responses,
154 including vasodilation and edema, via the G protein-triggered phosphatidylinositol-calcium
155 second messenger system.²²⁻²⁶

156 The fact that SARS-CoV-2 utilizes ACE2 to enter airway cells along with the fact that ACE2
157 is a multifunctional enzyme that counter-regulates the ACE-driven mechanisms of the RAS and
158 balances the KKS, may therefore explain the serious course of COVID-19, not only in the lungs
159 but systemically.^{27,28}

160 Recent publications suggest that the KKS could play a role in COVID-19. KKS comes into play
161 particularly in connection with the high prevalence of thromboembolic events in seriously ill
162 COVID-19 patients.^{7,18,20,29,30} A recent study on a cohort of 66 COVID-19 patients admitted to
163 the intensive care unit showed that the KKS was strongly activated, which was reflected in the
164 consumption of factor XII, pre-kallikrein and high-molecular-weight kininogen (HMW-
165 kininogen).²⁹ It has further been hypothesized that kinin-dependent “local lung angioedema”
166 involving the kinin B₁ and B₂ receptors is an important characteristic of COVID-19.³¹⁻³⁴

167 This study examines the potential of interfering with the KKS at the kinin receptor level in
168 SARS-CoV-2 infection with translational relevance. Based on a broad and strong upregulation
169 of kallikreins and of the kinin B₂ receptor in the nasal mucosa of acutely SARS-CoV-2-positive
170 patients, we hypothesized that the B₂ receptor antagonism using icatibant, an approved
171 compound for the treatment of hereditary angioedema,³⁵ had an early protective effect against
172 SARS-CoV-2-mediated epithelial damage through disruption of ACE2-mediated virus entry.

173

174 **2 MATERIALS AND METHODS**

175 **2.1 Patients and nasal brushings**

176 The nasal brushings were performed as a part of a larger health professional observational
177 cohort study, which was approved by the ethics commission of the Technical University of
178 Munich (AZ 175/20s). Nasal brushings were subjected to whole-genome microarray
179 transcriptome analysis (see Supp.Info.). All patients gave written, informed consent prior to
180 participation (see Table 1).

181

182 **2.2 *In vivo* mouse study**

183 Mice received murine IL-12Fc (1 µg of protein in 50 µL PBS) or PBS control intranasally.³⁶
184 Intranasal application was performed under isoflurane anesthesia in two steps of 25 µL per
185 nostril. 48 hours later, the mice received a single subcutaneous injection of icatibant (2 nmol
186 per 10 g body weight; HOE-140 (icatibant), H157, SLBX4410, Sigma) or PBS control. The
187 experiment was terminated by CO₂ asphyxiation 6 hours or 24 hours after the injection of
188 icatibant. The experiment was carried out twice. Organs were snap frozen for protein extraction.
189 Mice enrolled in the experiment were 6-8 weeks old, from either C57BL/6J, BALB/c or C3H
190 HeN strains. Both sexes were included for each strain and means of each mouse type (strain /
191 sex) are depicted as single values in Fig.2A: circle: female; triangle: male. Black: C57BL/6,
192 mid grey: C3H HeN, light grey: BALB/c strain. Experiments were performed and analyzed in
193 a randomized and blinded fashion. Animals were obtained from Janvier Labs (Le Genest-Saint-
194 Isle, France) and housed 5 per cage and sex in individually ventilated cages at Laboratory
195 Animal Service Center of the University of Zurich in Schlieren (Schlieren, Zurich,
196 Switzerland). The animal vivarium was a specific-pathogen-free (SPF) holding room, that was
197 temperature- and humidity-controlled (21 ± 3 °C, 50 ± 10%), with a 12h light/dark cycle. All
198 animals had ad libitum access to the same food and water throughout the entire study. All
199 procedures described in this study had previously been approved by the Cantonal Veterinarian's

200 Office of Zurich, Switzerland (License ZH096/20), and every effort was made to minimize the
201 number of animals used and their suffering. Experiments were pre-registered at
202 www.animalstudyregistry.org (study title "Effect of drug on ACE2 levels in mice";
203 doi=10.17590/asr.0000225).
204 Detailed methods are provided in the online supporting information.
205

206 3 RESULTS

207 3.1 B₂ receptor antagonist inhibits replication and spread of SARS-CoV-2

208 The enzyme ACE2 is the central viral entry receptor for the novel SARS-CoV-2 coronavirus
209 on human epithelial cells of the respiratory tract.¹⁰ Recent studies showed that this receptor and
210 its co-receptors are not only expressed in the lower respiratory tract, and thus on the alveolar
211 epithelial cells type I and II, but are also present in the upper respiratory tract, but are
212 predominantly expressed in the nasal mucosa.³⁷

213 To investigate the local effect of the acute SARS-CoV-2 infection on the nasal epithelium, we
214 analyzed the transcriptome of nasal brushings from symptomatic patients who tested acutely
215 positive for SARS-CoV-2 and of SARS-CoV-2-negative patients. In a transcriptome analysis,
216 the most strongly induced genes encoding secreted factors included many members of the
217 kallikrein family (Fig.1A, Table S1). In particular, the kallikreins *KLK5*, *KLK9* and *KLK12*
218 were significantly upregulated in acute SARS-CoV-2-positive patients compared to SARS-
219 CoV-2-negative patients (Fig.1B, Table S2). A subsequent analysis focusing on central factors
220 of the KKS revealed that in addition, the kinin receptor B₂ (*BDKRB2*; B₂R) was also
221 significantly increased (Fig.1C, Table S3). This first finding, together with our hypothesis that
222 ACE2, as a central component, is counter-regulated by intervention in the KKS, prompted us
223 to investigate selective kinin B₂ receptor antagonism in connection with SARS-CoV-2
224 infection. To circumvent the limitations of cell lines like Vero E6, A549 or Calu-3 cells that are
225 intrinsically impaired to form an interferon response upon viral infection,³⁸ we next infected
226 primary bronchial epithelial (NHBE) cells with SARS-CoV-2.

227 To examine the effects of SARS-CoV-2 infection and B₂R antagonist treatment on the
228 microscopic integrity of the airway epithelium, 3D-air-liquid interphase organoid cultures were
229 differentiated from primary NHBEs (see Supp.Info). After complete differentiation, the
230 epithelia were pre-treated from the basal (medium) side with the approved B₂R antagonist
231 icatibant, and subsequently infected with SARS-CoV-2 from the apical (air) side. The cultures

232 pre-treated with the B₂R antagonist showed less virus-induced balloon-like structures compared
233 to untreated cultures. The epithelial layers remained qualitatively more intact, which indicated
234 a protective effect of the B₂R antagonist for the bronchial epithelium (Fig.1D). This finding
235 was further strengthened by cytotoxicity assays: The B₂R antagonist had no toxic effects on
236 NHBEs even at high doses determined by lactate dehydrogenase (LDH) release, but rather
237 exhibited a cell-protecting effect in uninfected cells (Fig.1E) as well as during SARS-CoV-2
238 infection (Fig.1F). Next, the supernatants of pre-treated, infected primary NHBEs were
239 collected, titrated onto fresh Vero E6 cell cultures and plaque assays were performed.
240 Strikingly, we found that *in vitro* treatment of NHBEs with the B₂R antagonist prior to infection
241 reduced the number of plaque forming units (PFU) in a plaque assay by 87% (Fig.1G). In
242 addition, the levels of total SARS-CoV-2 RNA in cells that had been pretreated with the B₂R
243 antagonist decreased by 52% compared to untreated infected NHBEs (Fig.1H). With regard to
244 the virus entry process, ACE2 was reduced by pretreatment with the B₂R antagonist on the
245 mRNA level (Fig. 1I) and on the protein level (Fig. 1J). The membrane-standing protease
246 TMPRSS2 cleaves the spike protein for SARS-CoV-2 and primes it therefore for optimized
247 binding to its entry receptor ACE2. In contrast to ACE2, the *TMPRSS2* transcript levels were
248 significantly increased in infected compared to uninfected NHBEs but were not affected by
249 B₂R antagonist pre-treatment (Fig.S2A). Further experiments on the effect of the B₂R
250 antagonist on the SARS-CoV-2 infection of NHBE showed that pre-treatment with the B₂R
251 antagonist significantly reduced infection-mediated cytotoxicity measured by LDH release
252 (Fig.1F).

253

254 **3.2 Repetitive treatment with B₂R antagonist inhibits SARS-CoV-2 replication and spread** 255 **post-infection**

256 The finding that B₂R antagonism leads to a downregulation of ACE2 protein levels in lung
257 epithelial cells was confirmed *in vivo* in a murine airway inflammation model. 24 sex-matched

258 mice from three different strains per group were treated in two blocks intranasally with murine
259 IL-12Fc to mimic virus-induced airway inflammation via activation of the IL-12 / IFN- γ axis.³⁶
260 After 48 hours, mice were injected subcutaneously (s.c.) with the B₂R antagonist and the
261 experiment was terminated six hours or 24 hours later. IL-12Fc-pretreated mice, which were
262 then further treated with the B₂R antagonist on day 2, had significantly reduced ACE2 protein
263 levels in the lungs after six hours compared to control mice, which were only treated with PBS
264 on day 2 (Fig.2A). This effect decreased after 24 hours.

265 Anticipating treatment of SARS-CoV-2 infected patients with the B₂R antagonist icanitabant,
266 NHBEs were first infected with SARS-CoV-2 and then treated with the B₂R antagonist six
267 hours after infection. Confirming the results of the pre-treatment, post-infection treatment with
268 the B₂R antagonist also attenuated the cytopathic effect of SARS-CoV-2 (Fig.2B) and reduced
269 the number of PFU in a plaque assay on Vero E6 cells by 84% (Fig.2C).

270 We also aimed to reflect pharmacokinetics³⁹ during treatment of early infection by treating
271 NHBEs post-infection every 24 hours with the B₂R antagonist repeatedly for a period of 96
272 hours, reflecting the drug administration of this particular substance in real life. In cells treated
273 post-infection with 100 nM icanitabant for 48 hours, the total viral RNA (Fig.2D-F IC₅₀(total
274 RNA 48h)=92.93; IC₅₀(total RNA 72h)=91.56) and also the genomic viral RNA (Fig.2G-I;
275 IC₅₀(total RNA 48h)=17.01; IC₅₀(total RNA 72h)=7.412) were significantly reduced by 49%
276 and 42% on average, respectively. Treatment with 1000 nM icanitabant for 48 hours led to a
277 reduction of the total SARS-CoV-2 RNA (Fig.2D-F) and also of the genomic SARS-CoV-2
278 RNA (Fig.2G-I) by 69% and 56% on average, respectively. The genomic viral RNA was
279 detected using RT-qPCR against the sequence of the SARS-CoV-2 RNA-dependent RNA
280 polymerase (*RdRP*), which is only found in virions as well as during the viral replication. On
281 the other hand, total viral RNA was detected with qPCR targeting a sequence of the SARS-
282 CoV-2 *N* gene that is present in the viral genome and also in every SARS-CoV-2 protein-
283 encoding transcript. The reduction in total SARS-CoV-2 RNA and genomic viral RNA during

284 treatment with the B₂R antagonist was comparable at the indicated concentrations and time
285 points (Fig.2D-I).

286

287 **3.3 B₂ receptor antagonism broadly silences gene expression in bronchial epithelial cells** 288 **while maintaining cell-intrinsic antiviral response**

289 Severe cases of COVID-19 develop cytokine storms⁴⁰⁻⁴² characterized by excessive systemic
290 release of multiple cytokines including IP-10 (*CXCL10*), IL-6, IL-8 (*CXCL8*), and IL-10.⁴³⁻⁴⁶

291 These cases are currently treated with immunomodulating drugs, such as corticosteroids or
292 biologics, like tocilizumab⁴⁷, though these treatments may interfere with or alter the antiviral

293 immune response. We therefore compared the effect of the B₂R antagonist on gene expression
294 of the bronchial epithelium in the light of SARS-CoV-2 infection with the effect of

295 hydrocortisone. While the B₂R antagonist mainly suppressed epithelial gene expression during
296 infection, the effects of hydrocortisone on gene induction and gene repression were equal

297 (Fig.3A, Tables S4-5). This finding matches previous reports.⁴⁸ Therefore, conditions were

298 compared in respect to the antiviral epithelial response. In fact, differentially expressed genes
299 (DEGs) induced by SARS-CoV-2 infection in NHBEs encompassed type-I and -III interferons

300 as well as IFN-inducible and antiviral *APOBEC* genes (Fig.S1E, Table S6). In particular,

301 SARS-CoV-2 infection induced the antiviral cytidine deaminases APOBEC3A and B, which
302 we previously described to be induced by type-I interferons in the treatment of hepatitis-B virus

303 infection.⁴⁹ On the other hand, *APOBEC3C* mRNA levels were decreased in SARS-CoV-2-

304 infected NHBE, which could indicate a novel evasion mechanism.⁵⁰ Neither the B₂R antagonist

305 nor hydrocortisone inhibited the expression of genes with cell-intrinsic antiviral effects and
306 even increased the antiviral factor *APOBEC3A* at the mRNA level (Fig.3B, Table S7).⁵¹

307 Our gene expression analysis data show that SARS-CoV-2 infection also induces the expression
308 of acute-phase proteins, such as TNF- α and IL-8 (*CXCL8*),^{52,53} as well as IL-17C, MIP-

309 3 α (*CCL20*), IL-36 γ ^{54,55} and the chemokines CXCL1, -2, -3, -8, -17, CCL2, -3, -5⁵⁴ in primary

310 lung epithelial cells (Fig.3C, Table S8). The induction of these factors most likely contributes
311 to the recruitment and activation of relevant immune cells to the site of infection. Our findings
312 are supported by previous studies of aberrant macrophage and T cell responses underlying
313 immunopathogenesis in bronchoalveolar lavage fluid from COVID-19 patients.⁵⁶ In addition,
314 the gene expression of acute-phase proteins was not significantly affected in airway epithelial
315 cells by the B₂R antagonist or hydrocortisone treatment (Fig.3C, Table S8). Neither drug
316 interfered with canonical cellular antiviral – and reaction-triggering response mechanisms,
317 showing great potential for treatment options of COVID-19 while maintaining the host’s
318 antiviral immune response.

319 In addition, we found that SARS-CoV-2 infection increases the expression of three known and
320 postulated entry (co-)receptors: 1) the transmembrane serine protease TMPRSS11A (Fig.S1C,
321 Tables S6,9-13), which was described to prime the MERS coronavirus spike protein⁵⁷, 2) the
322 transmembrane serine protease TMPRSS11D, which was shown to activate SARS-CoV-2 spike
323 protein⁵⁸ and 3) the pathogen-associated molecular pattern-binding C-type lectin receptor DC-
324 SIGN (*CD209*), which was described to serve as entry receptor for SARS-CoV⁵⁹ and has been
325 suggested to act as a receptor also for SARS-CoV-2. The induction of these additional entry
326 receptor candidates triggered by SARS-CoV-2 infection may potentiate the viral spread in the
327 bronchial epithelium and thus represent a pathogenetic approach that needs further research.

328 Overall, treatment with the B₂R antagonist and hydrocortisone had no significant effects on the
329 expression of these candidate viral entry receptors (Fig.3D, Table S14). On the other hand,
330 hydrocortisone enhanced the expression of TMPRSS proteases (Fig.3D). In particular, when
331 focusing on the known SARS-CoV-2 entry receptors, hydrocortisone treatment of uninfected
332 cells was already sufficient to induce an increase in *TMPRSS2* gene expression (Fig.3E). SARS-
333 CoV-2 infection per se also increased *TMPRSS2* expression, and pre-treatment of SARS-CoV-
334 2-infected NHBEs with hydrocortisone further potentiated this effect. On the other hand, *ACE2*
335 expression showed only a slight upward trend after hydrocortisone pretreatment (Fig.S2B).

336 Finally, the hydrocortisone pre-treatment of SARS-CoV-2-infected NHBEs had no inhibitory
337 effect on the release of infectious particles 24 hours after infection (Fig.3F), which was
338 expected since the treatment of COVID-19 patients with corticosteroids has an
339 immunomodulatory rationale.

340

341 **3.4 B₂ receptor antagonist counter-balances virus-induced gene expression, particularly** 342 **genes involved in G protein-coupled receptor (GPCR) signaling and ion transport**

343 With regard to the genes that are attenuated at the mRNA level by B₂R antagonism, the DEGs
344 were analyzed in a network analysis using the database string to identify enriched cellular
345 processes. B₂R antagonism reduced the expression levels of 343 membrane-bound receptors
346 significantly in treated versus untreated SARS-CoV-2-infected NHBEs (Table S15). Two
347 particular cellular processes affected by pre-treatment with the B₂R antagonist were identified,
348 namely G protein-coupled receptor signaling (GO:0007186; Fig.4A, S2C, Tables S4,S17-18)
349 and ion transport (GO:0006811; Fig.4B, Tables S4,17-18). DEGs involved in both processes
350 were significantly downregulated in treated versus untreated SARS-CoV-2-infected NHBEs
351 (Tables 16-18). Notably, all 35 cell surface receptors induced by SARS-CoV-2 infection were
352 downregulated in cells that were treated with the B₂R antagonist (Fig.4C,D, Tables S19-20).

353

354

355 **4 DISCUSSION**

356 In this study, we provide evidence for the effect of interference with the KKS at the kinin B₂
357 receptor level as a means of protecting the airway epithelium from SARS-CoV-2 infection,
358 while maintaining canonical cell-intrinsic antiviral response.

359 We initially hypothesized that through KKS interference, either feedback mechanisms or
360 modulated signal transduction target the virus entry receptor ACE2 and thus interfere with the
361 spread of SARS-CoV-2. To this end, the approved B₂R antagonist icatibant was used in this
362 study. Here, we demonstrate that treatment with a B₂R antagonist inhibits the replication and
363 spread of SARS-CoV-2 in primary airway epithelial cells, which was determined by a decrease
364 in total and genomic SARS-CoV-2 RNA, resulting in less infectious particles in plaque assays,
365 both when applied pre- and post-infection. While a low concentration of 1 nM B₂R antagonist
366 was sufficient to reduce viral RNA in primary bronchial epithelial cells when cells were treated
367 pre-infection, 100 nM B₂R antagonist was required to this effect, when cells were treated post-
368 infection. In addition, the significant reduction in virus load as determined by PCR tapered off
369 after 96 hours. On the one hand, *in vitro* infections are performed with excess amounts of virus
370 particles. On the other hand, the fact that, due to its constitution as a peptide analog, the B₂R
371 antagonist icatibant used in this study has a short half-life in the human body³⁹ but also
372 pharmacological tolerance to interference at receptor level may explain why the effect reached
373 significance after six hours but did not persist. Therefore, a higher dose of the B₂R antagonist
374 may be required at even shorter repetitive dosing intervals to inhibit virus replication in the long
375 term. Therapeutic application in future dose finding studies should therefore focus on early
376 intervention with at least two doses daily⁶⁰ and on either optimized pharmacokinetics or
377 increased high local tissue concentrations, e.g. through topical application.

378

379 Two potential mechanisms of action for suppressing SARS-CoV-2 replication and spread in
380 airway epithelium are revealed by the current study:

381 1) Treatment with the B₂R antagonist led to a downregulation of the viral entry receptor ACE2,
382 *in vitro* in primary airway epithelial cells and *in vivo* in a murine airway inflammation model.
383 Since the decrease of genomic SARS-CoV-2 RNA and total SARS-CoV-2 RNA was
384 comparable, we conclude that the B₂R antagonist icatibant does probably not affect the viral
385 transcription machinery but inhibits the infection rather on the levels of entry, protein
386 synthesis/processing and assembly, maturation or budding.

387 In comparison, the corticosteroid hydrocortisone even upregulated TMPRSS2 in infected
388 airway epithelial cells. It is noteworthy that hydrocortisone did not change the release of
389 infectious particles from infected airway epithelial cells into the supernatant. Although
390 TMPRSS2 expression was even enhanced by hydrocortisone, our data implicate that this effect
391 on TMPRSS2 alone is insufficient to increase susceptibility for SARS-CoV-2 infection.

392 2) Treatment with the B₂R antagonist had a broad suppressive effect on gene expression of
393 multiple cell signaling molecules, in particular on membrane-standing factors involved in
394 GPCR signaling and ion transport.

395 It has recently been published that SARS-CoV-2 may use cellular GPCR signaling pathways,
396 thereby modulate epithelial transport mechanisms involved in ion transport and thereby cause
397 a local ion imbalance in the airways.⁶¹ In addition, an extensive recent study described that
398 intracellular SARS-CoV-2 protein interactions include factors involved in intracellular
399 trafficking and transport, particularly ion transport and solute carrier transport.⁶² In fact, the
400 SARS-CoV-2 infection led to a differential regulation of the gene expression of 12 potassium
401 channel (5 upregulated / 7 downregulated), 1 sodium channel (down), but in particular of 55
402 members of the solute carrier family (24 downregulated / 31 upregulated) in primary airway
403 epithelial cells. On the other hand, B₂R antagonist treatment of SARS-CoV-2-infected NHBE
404 resulted in a downregulation of 20 potassium channel genes and 6 sodium channel genes, as
405 well as a downregulation of 29 members of the solute carrier family.

406 We therefore conclude that B₂R antagonism not only impedes the viral entry process by
407 reducing ACE2, as we had hypothesized, but also counter-regulates cellular processes that
408 include GPCR signaling and transmembrane ion transport, which SARS-CoV-2 may utilize for
409 efficient replication and viral spread.

410
411 In conclusion, the results of this study suggest that B₂ receptor-antagonism protects airway
412 epithelial cells from SARS-CoV-2 spread by reducing ACE2 levels and by interfering with
413 several cellular signaling processes. Further research is needed to elucidate more details about
414 molecular mechanisms involved in the viral life cycle that kinin B₂ receptor antagonism targets
415 and underlie its effects against SARS-CoV-2 infection. Based on these data, we speculate that
416 the protective effects of B₂R antagonism could potentially prevent the early stages of COVID-
417 19 from progressing into severe acute respiratory distress syndrome (ARDS) with structural
418 airway damage and fibrotic changes. We therefore propose that the safe approved B₂R
419 antagonist icatibant be tested in clinical trials for two important aspects: 1) Treatment of early
420 COVID-19 disease targeting the replication and spread of the virus. 2) Optimized dosage
421 regimen to reflect pharmacokinetics and possible pharmacological tolerance at the receptor
422 level. Future controlled clinical trials must provide substantial evidence for optimal dosage
423 regimen, application, efficacy, and safety to investigate, whether KKS interference at the kinin
424 B₂ receptor level can prevent the escalation of COVID-19 to ARDS and long-term lung damage.
425

426 REFERENCES

- 427 1. Polack FP, Thomas SJ, Kitchin N, et al. Safety and Efficacy of the BNT162b2 mRNA
428 Covid-19 Vaccine. *N Engl J Med.* 2020;383(27):2603-2615.
- 429 2. Zhang JJ, Dong X, Cao YY, et al. Clinical characteristics of 140 patients infected with
430 SARS-CoV-2 in Wuhan, China. *Allergy.* 2020;75(7):1730-1741.
- 431 3. Planas D, Veyer D, Baidaliuk A, et al. Reduced sensitivity of SARS-CoV-2 variant
432 Delta to antibody neutralization. *Nature.* 2021.
- 433 4. Hacisuleyman E, Hale C, Saito Y, et al. Vaccine Breakthrough Infections with SARS-
434 CoV-2 Variants. *N Engl J Med.* 2021.
- 435 5. Schmidt F, Weisblum Y, Muecksch F, et al. Measuring SARS-CoV-2 neutralizing
436 antibody activity using pseudotyped and chimeric viruses. *J Exp Med.* 2020;217(11).
- 437 6. Sokolowska M, Lukasik ZM, Agache I, et al. Immunology of COVID-19: Mechanisms,
438 clinical outcome, diagnostics, and perspectives-A report of the European Academy of
439 Allergy and Clinical Immunology (EAACI). *Allergy.* 2020;75(10):2445-2476.
- 440 7. Gao YD, Ding M, Dong X, et al. Risk factors for severe and critically ill COVID-19
441 patients: A review. *Allergy.* 2021;76(2):428-455.
- 442 8. Bousquet J, Jutel M, Akdis CA, et al. ARIA-EAACI statement on asthma and COVID-
443 19 (June 2, 2020). *Allergy.* 2021;76(3):689-697.
- 444 9. Du H, Dong X, Zhang JJ, et al. Clinical characteristics of 182 pediatric COVID-19
445 patients with different severities and allergic status. *Allergy.* 2021;76(2):510-532.
- 446 10. Hoffmann M, Kleine-Weber H, Schroeder S, et al. SARS-CoV-2 Cell Entry Depends
447 on ACE2 and TMPRSS2 and Is Blocked by a Clinically Proven Protease Inhibitor. *Cell.*
448 2020;181(2):271-280 e278.
- 449 11. Matsuyama S, Nagata N, Shirato K, Kawase M, Takeda M, Taguchi F. Efficient
450 activation of the severe acute respiratory syndrome coronavirus spike protein by the
451 transmembrane protease TMPRSS2. *J Virol.* 2010;84(24):12658-12664.
- 452 12. Li W, Moore MJ, Vasileva N, et al. Angiotensin-converting enzyme 2 is a functional
453 receptor for the SARS coronavirus. *Nature.* 2003;426(6965):450-454.
- 454 13. Diamond B. The renin-angiotensin system: An integrated view of lung disease and
455 coagulopathy in COVID-19 and therapeutic implications. *J Exp Med.* 2020;217(8).
- 456 14. Schmaier AH. The contact activation and kallikrein/kinin systems: pathophysiologic
457 and physiologic activities. *J Thromb Haemost.* 2016;14(1):28-39.
- 458 15. Stukalov A, Girault V, Grass V, et al. Multilevel proteomics reveals host perturbations
459 by SARS-CoV-2 and SARS-CoV. *Nature.* 2021.
- 460 16. Imai Y, Kuba K, Rao S, et al. Angiotensin-converting enzyme 2 protects from severe
461 acute lung failure. *Nature.* 2005;436(7047):112-116.
- 462 17. Santos RAS, Sampaio WO, Alzamora AC, et al. The ACE2/Angiotensin-(1-7)/MAS
463 Axis of the Renin-Angiotensin System: Focus on Angiotensin-(1-7). *Physiol Rev.*
464 2018;98(1):505-553.
- 465 18. Meini S, Zanichelli A, Sbrojavacca R, et al. Understanding the Pathophysiology of
466 COVID-19: Could the Contact System Be the Key? *Front Immunol.* 2020;11:2014.
- 467 19. Vickers C, Hales P, Kaushik V, et al. Hydrolysis of biological peptides by human
468 angiotensin-converting enzyme-related carboxypeptidase. *J Biol Chem.*
469 2002;277(17):14838-14843.
- 470 20. van de Veerdonk FL, Netea MG, van Deuren M, et al. Kallikrein-kinin blockade in
471 patients with COVID-19 to prevent acute respiratory distress syndrome. *Elife.* 2020;9.
- 472 21. Shen B, Harrison-Bernard LM, Fuller AJ, Vanderpool V, Saifudeen Z, El-Dahr SS. The
473 Bradykinin B2 receptor gene is a target of angiotensin II type 1 receptor signaling. *J Am*
474 *Soc Nephrol.* 2007;18(4):1140-1149.

- 475 22. Burch RM, Axelrod J. Dissociation of bradykinin-induced prostaglandin formation
476 from phosphatidylinositol turnover in Swiss 3T3 fibroblasts: evidence for G protein
477 regulation of phospholipase A2. *Proc Natl Acad Sci U S A.* 1987;84(18):6374-6378.
- 478 23. Slivka SR, Insel PA. Phorbol ester and neomycin dissociate bradykinin receptor-
479 mediated arachidonic acid release and polyphosphoinositide hydrolysis in Madin-Darby
480 canine kidney cells. Evidence that bradykinin mediates noninterdependent activation of
481 phospholipases A2 and C. *J Biol Chem.* 1988;263(29):14640-14647.
- 482 24. Yu HS, Lin TH, Tang CH. Involvement of intercellular adhesion molecule-1 up-
483 regulation in bradykinin promotes cell motility in human prostate cancers. *Int J Mol Sci.*
484 2013;14(7):13329-13345.
- 485 25. Chen S, Zhang L, Xu R, et al. BDKRB2 +9/-9 bp polymorphisms influence BDKRB2
486 expression levels and NO production in knee osteoarthritis. *Exp Biol Med (Maywood).*
487 2017;242(4):422-428.
- 488 26. Souza PPC, Lundberg P, Lundgren I, Magalhaes FAC, Costa-Neto CM, Lerner UH.
489 Activation of Toll-like receptor 2 induces B1 and B2 kinin receptors in human gingival
490 fibroblasts and in mouse gingiva. *Sci Rep.* 2019;9(1):2973.
- 491 27. Imai Y, Kuba K, Penninger JM. The discovery of angiotensin-converting enzyme 2 and
492 its role in acute lung injury in mice. *Exp Physiol.* 2008;93(5):543-548.
- 493 28. Jia H. Pulmonary Angiotensin-Converting Enzyme 2 (ACE2) and Inflammatory Lung
494 Disease. *Shock.* 2016;46(3):239-248.
- 495 29. Lipcsey M, Persson B, Eriksson O, et al. The Outcome of Critically Ill COVID-19
496 Patients Is Linked to Thromboinflammation Dominated by the Kallikrein/Kinin System.
497 *Front Immunol.* 2021;12:627579.
- 498 30. Mansour E, Palma AC, Ulaf RG, et al. Safety and Outcomes Associated with the
499 Pharmacological Inhibition of the Kinin-Kallikrein System in Severe COVID-19.
500 *Viruses.* 2021;13(2).
- 501 31. de Maat S, de Mast Q, Danser AHJ, van de Veerdonk FL, Maas C. Impaired Breakdown
502 of Bradykinin and Its Metabolites as a Possible Cause for Pulmonary Edema in COVID-
503 19 Infection. *Semin Thromb Hemost.* 2020;46(7):835-837.
- 504 32. Garvin MR, Alvarez C, Miller JI, et al. A mechanistic model and therapeutic
505 interventions for COVID-19 involving a RAS-mediated bradykinin storm. *Elife.*
506 2020;9.
- 507 33. Kaplan AP, Ghebrehiwet B. Pathways for bradykinin formation and interrelationship
508 with complement as a cause of edematous lung in COVID-19 patients. *J Allergy Clin*
509 *Immunol.* 2021;147(2):507-509.
- 510 34. Roche JA, Roche R. A hypothesized role for dysregulated bradykinin signaling in
511 COVID-19 respiratory complications. *FASEB J.* 2020;34(6):7265-7269.
- 512 35. Bas M, Bier H, Greve J, Kojda G, Hoffmann TK. Novel pharmacotherapy of acute
513 hereditary angioedema with bradykinin B2-receptor antagonist icatibant. *Allergy.*
514 2006;61(12):1490-1492.
- 515 36. Eisenring M, vom Berg J, Kristiansen G, Saller E, Becher B. IL-12 initiates tumor
516 rejection via lymphoid tissue-inducer cells bearing the natural cytotoxicity receptor
517 NKp46. *Nat Immunol.* 2010;11(11):1030-1038.
- 518 37. Sungnak W, Huang N, Becavin C, et al. SARS-CoV-2 entry factors are highly expressed
519 in nasal epithelial cells together with innate immune genes. *Nat Med.* 2020;26(5):681-
520 687.
- 521 38. Yoshikawa T, Hill TE, Yoshikawa N, et al. Dynamic innate immune responses of
522 human bronchial epithelial cells to severe acute respiratory syndrome-associated
523 coronavirus infection. *PLoS One.* 2010;5(1):e8729.
- 524 39. Leach JK, Spencer K, Mascelli M, McCauley TG. Pharmacokinetics of single and
525 repeat doses of icatibant. *Clin Pharmacol Drug Dev.* 2015;4(2):105-111.

- 526 40. Huang C, Wang Y, Li X, et al. Clinical features of patients infected with 2019 novel
527 coronavirus in Wuhan, China. *Lancet*. 2020;395(10223):497-506.
- 528 41. Zhou F, Yu T, Du R, et al. Clinical course and risk factors for mortality of adult
529 inpatients with COVID-19 in Wuhan, China: a retrospective cohort study. *Lancet*.
530 2020;395(10229):1054-1062.
- 531 42. Burian E, Jungmann F, Kaissis GA, et al. Intensive Care Risk Estimation in COVID-19
532 Pneumonia Based on Clinical and Imaging Parameters: Experiences from the Munich
533 Cohort. *J Clin Med*. 2020;9(5).
- 534 43. Zheng HY, Zhang M, Yang CX, et al. Elevated exhaustion levels and reduced functional
535 diversity of T cells in peripheral blood may predict severe progression in COVID-19
536 patients. *Cell Mol Immunol*. 2020.
- 537 44. Laing AG, Lorenc A, Del Molino Del Barrio I, et al. A dynamic COVID-19 immune
538 signature includes associations with poor prognosis. *Nat Med*. 2020;26(10):1623-1635.
- 539 45. Buszko M, Nita-Lazar A, Park JH, et al. Lessons learned: new insights on the role of
540 cytokines in COVID-19. *Nat Immunol*. 2021;22(4):404-411.
- 541 46. Azkur AK, Akdis M, Azkur D, et al. Immune response to SARS-CoV-2 and
542 mechanisms of immunopathological changes in COVID-19. *Allergy*. 2020;75(7):1564-
543 1581.
- 544 47. Group RC. Tocilizumab in patients admitted to hospital with COVID-19
545 (RECOVERY): a randomised, controlled, open-label, platform trial. *Lancet*.
546 2021;397(10285):1637-1645.
- 547 48. Mostafa MM, Rider CF, Shah S, et al. Glucocorticoid-driven transcriptomes in human
548 airway epithelial cells: commonalities, differences and functional insight from cell lines
549 and primary cells. *BMC Med Genomics*. 2019;12(1):29.
- 550 49. Lucifora J, Xia Y, Reisinger F, et al. Specific and nonhepatotoxic degradation of nuclear
551 hepatitis B virus cccDNA. *Science*. 2014;343(6176):1221-1228.
- 552 50. Milewska A, Kindler E, Vkovski P, et al. APOBEC3-mediated restriction of RNA virus
553 replication. *Sci Rep*. 2018;8(1):5960.
- 554 51. Wang Y, Schmitt K, Guo K, Santiago ML, Stephens EB. Role of the single deaminase
555 domain APOBEC3A in virus restriction, retrotransposition, DNA damage and cancer.
556 *J Gen Virol*. 2016;97(1):1-17.
- 557 52. Rodgers HC, Pang L, Holland E, Corbett L, Range S, Knox AJ. Bradykinin increases
558 IL-8 generation in airway epithelial cells via COX-2-derived prostanoids. *Am J Physiol*
559 *Lung Cell Mol Physiol*. 2002;283(3):L612-618.
- 560 53. Norelli M, Camisa B, Barbiera G, et al. Monocyte-derived IL-1 and IL-6 are
561 differentially required for cytokine-release syndrome and neurotoxicity due to CAR T
562 cells. *Nat Med*. 2018;24(6):739-748.
- 563 54. Tay MZ, Poh CM, Renia L, MacAry PA, Ng LFP. The trinity of COVID-19: immunity,
564 inflammation and intervention. *Nat Rev Immunol*. 2020.
- 565 55. Merad M, Martin JC. Pathological inflammation in patients with COVID-19: a key role
566 for monocytes and macrophages. *Nat Rev Immunol*. 2020.
- 567 56. Mingfeng Liao YL, Jing Yuan, Yanling Wen, Gang Xu, Juanjuan Zhao, Lin Cheng,
568 Jinxiu Li, Xin Wang, Fuxiang Wang, Lei Liu, Ido Amit, Shuye Zhang & Zheng Zhang.
569 Single-cell landscape of bronchoalveolar immune cells in patients with COVID-19. *Nat*
570 *Med*. 2020.
- 571 57. Zmora P, Hoffmann M, Kollmus H, et al. TMPRSS11A activates the influenza A virus
572 hemagglutinin and the MERS coronavirus spike protein and is insensitive against
573 blockade by HAI-1. *J Biol Chem*. 2018;293(36):13863-13873.
- 574 58. Kishimoto M, Uemura K, Sanaki T, et al. TMPRSS11D and TMPRSS13 Activate the
575 SARS-CoV-2 Spike Protein. *Viruses*. 2021;13(3).

- 576 59. Han DP, Lohani M, Cho MW. Specific asparagine-linked glycosylation sites are critical
577 for DC-SIGN- and L-SIGN-mediated severe acute respiratory syndrome coronavirus
578 entry. *J Virol.* 2007;81(21):12029-12039.
- 579 60. van de Veerdonk FL, Kouijzer IJE, de Nooijer AH, et al. Outcomes Associated With
580 Use of a Kinin B2 Receptor Antagonist Among Patients With COVID-19. *JAMA Netw*
581 *Open.* 2020;3(8):e2017708.
- 582 61. Abdel Hameid R, Cornet-Boyaka E, Kuebler WM, Uddin M, Berdiev BK. SARS-CoV-
583 2 may hijack GPCR signaling pathways to dysregulate lung ion and fluid transport. *Am*
584 *J Physiol Lung Cell Mol Physiol.* 2021;320(3):L430-L435.
- 585 62. Stukalov A, Girault V, Grass V, et al. Multilevel proteomics reveals host perturbations
586 by SARS-CoV-2 and SARS-CoV. *Nature.* 2021;594(7862):246-252.
587

588 **FIGURE LEGENDS**

589 **Figure 1. Induction of kallikreins and kinin receptor B₂ in the nasal mucosa of acutely**
590 **positive Covid-19 patients**

591 A) Volcano plot of significantly differentially regulated genes (DEGs = differentially expressed
592 genes) in nasal brushings of patients that were acute positive for SARS-CoV-2 compared to
593 healthy individuals (negative) using human miR microarray technology. Highlighted genes
594 have a fold-change (FC) ≥ 10 with $P < 0.05$, genes in red are up-regulated, genes in blue are
595 downregulated. B) Heat map of gene expression analysis of kallikrein genes and C) of genes of
596 the kinin-kallikrein system (KKS) in nasal brushings comparing SARS-CoV-2 acute-positive
597 patients to healthy controls. All entities with $FC \geq 1.2$ are shown. Asterisks indicate significantly
598 regulated genes ($P < 0.05$) in SARS-CoV-2-infected NHBEs compared to medium. Color code
599 indicates Log₂-fold change from low (blue) through 0 (white) to high (red). Duplicate gene
600 names indicate the abundance of two or more isoforms of the same gene in the analysis. D) 3D-
601 air-liquid interphase cultures from NHBEs were pre-treated for 24 hours with/without 1 nM
602 B₂R antagonist from the basal side and subsequently infected with SARS-CoV-2 for 48 hours
603 from the apical side.

604 E) Lactate dehydrogenase (LDH) cytotoxicity assay using the LDH Cytotoxicity Detection Kit
605 PLUS studying the effect of increasing doses of the B₂R antagonist after 48 hours in primary
606 NHBEs from 4 donors. Results are depicted as mean \pm s.e.m. Statistical tests compared each
607 dose of B₂R antagonist with 0 nM B₂R antagonist.

608 F) Cytotoxicity assay determining LDH release into the supernatants of cultures of SARS-CoV-
609 2-infected NHBEs from 12 donors that were pre-treated for 24 hours with/without 1 nM B₂R
610 antagonist.

611 G) Quantification of infectious particles in the supernatants of SARS-CoV-2-infected NHBEs
612 from 10 donors that were pre-treated with/without 1 nM B₂R antagonist for 24 hours.
613 Supernatants were titrated on Vero E6 cells and plaque assay was quantified 24 hours later.

614 Results are depicted as plaque forming units (PFU) per milliliter.

615 H) qPCR analysis of total SARS-CoV-2 RNA (viral genome and transcripts, which all contain
616 the N1 sequence region) normalized to human *ACTB* of SARS-CoV-2-infected primary NHBE
617 after 24 hours of pre-treatment with/without 1 nM B₂R antagonist followed by 24 hours of
618 SARS-CoV-2 inoculation. For Figures 1E, F, and H, statistical tests compared SARS-CoV-2-
619 infected versus uninfected samples or B₂R antagonist-treated versus untreated samples.

620 I) Analysis of human ACE2 gene expression using qPCR (n=10) and J) of human ACE2 protein
621 levels analyzed by ELISA from cell lysates (n=6) after 24 hours of pre-treatment of NHBEs
622 with/without 1 nM B₂R antagonist, followed by SARS-CoV-2 inoculation for 24 hours.

623

624 **Figure 2. Treatment of NHBE with B₂R antagonist post-infection in repeated doses**
625 **inhibits SARS-CoV-2 replication**

626 A) *In vivo* mouse study. 12 sex-matched mice from three different strains per group were treated
627 on day 0 with intranasal application of 1 µg murine IL-12Fc per mouse or PBS as control to
628 mimic virus-induced airway inflammation. After 48h, mice were injected s.c. with 2 nmol of
629 the B₂R antagonist icatibant per 10 g of body weight or PBS as control. The experiment was
630 terminated either six hours or 24 hours later and murine lung ACE2 protein levels were
631 analyzed by mouse ACE2 ELISA analysis. Circle: female; triangle: male. Black: C57BL/6, mid
632 grey: C3H HeN, light grey: BALB/c strain. The experiment was carried out twice and the data
633 in the figure represent the mean of each mouse type (strain / sex) of both experiments. Statistical
634 tests compared B₂R antagonist -treated versus untreated groups.

635 B) Cytotoxicity assay determining LDH in supernatants from SARS-CoV-2-infected NHBEs
636 from 12 donors that were treated with/without 1 nM B₂R antagonist after 6 hours of infection
637 for another 24 hours. C) Quantification of infectious particles in the supernatants from SARS-
638 CoV-2-infected NHBEs from 4 donors that were treated with/without 1 nM B₂R antagonist
639 after 6 hours of infection for another 24 hours. Supernatants were titrated on Vero E6 cells and

640 plaque assay was quantified 24 hours later. Results are depicted as plaque forming units (PFU)
641 per milliliter. For Figures 2B-C, statistical tests compared B₂R antagonist-treated versus
642 untreated samples.

643 D) Relative quantification of total SARS-CoV-2 RNA (viral genome and transcripts, which all
644 contain the N1 sequence region) and G) genomic SARS-CoV-2 RNA (containing the *RdRP*
645 gene) normalized to housekeeping gene index of human *ACTB*, *HPRT*, *18S* in NHBEs from 8
646 independent donors that were infected with SARS-CoV-2 for 6 hours and then treated with
647 increasing doses of the B₂R antagonist icatibant repeatedly every 24 hours for a total of 96
648 hours. In cells treated with E) 100 nM and F) 1000 nM icatibant for 48 hours and with H) 100
649 nM and I) 1000 nM icatibant for 72 hours, total SARS-CoV-2 RNA and genomic SARS-CoV-
650 2 RNA were significantly reduced. Red indicates SARS-CoV-2 infection; blue indicates B₂R
651 antagonist treatment. PRE indicates pre-treatment; POST indicates post-treatment. In Fig.2D-
652 I, results are depicted as mean \pm s.e.m. and statistical tests compared each dose of icatibant with
653 0 nM icatibant. Statistically significant differences were depicted as p-values *P<0.05,
654 **P<0.01, and ***P<0.001. ns indicates non-significant. + infected / treated; - indicates not
655 infected / not treated.

656

657 **Figure 3. B₂R antagonism exhibits a protective and suppressive effect on gene expression**
658 **profile of airway epithelial cells.**

659 A) Volcano plots showing global gene expression changes induced by either treatment with
660 B₂R antagonist or hydrocortisone (HC). Red indicates significantly upregulated entities; blue
661 indicates significantly downregulated entities. Gene expression analysis of pre-treated NHBEs
662 after 24 hours of SARS-CoV-2 infection. B) Heat map of gene expression analysis of genes
663 involved in the epithelial antiviral response, analysis of the effects of SARS-CoV-2 infection.
664 Only entities with significant changes between SARS-CoV-2 infection and medium are shown
665 (gene expression fold change FC \geq 1.5 with P<0.05). C) Heat map of gene expression analysis

666 of genes involved in the acute phase response are depicted. All entities are shown. Asterisks
667 indicate significantly regulated genes ($P < 0.05$) in SARS-CoV-2 compared to medium. D) Heat
668 map of gene expression analysis of known and potential virus entry receptors are depicted. All
669 entities are shown. Color code indicates Log₂-fold change from low (blue) through 0 (white)
670 to high (red). Asterisks indicate significantly regulated genes ($P < 0.05$) in SARS-CoV-2-
671 infected NHBEs compared to medium. Duplicate gene names indicate the presence of two or
672 more isoforms of the same gene in the analysis. E) Analysis of *TMPRSS2* gene expression by
673 qPCR after 24 hours of pre-treatment with/without 10 μ M hydrocortisone (HC) followed by 24
674 hours of SARS-CoV-2 inoculation. Red indicates SARS-CoV-2 infection; yellow indicates pre-
675 treatment with hydrocortisone (HC). Statistical tests compared SARS-CoV-2-infected versus
676 uninfected samples or B₂R antagonist-treated versus untreated samples.

677 F) Quantification of infectious particles in the supernatants of SARS-CoV-2-infected NHBEs
678 from 10 donors that were pre-treated with/without 10 μ M hydrocortisone (HC) for 24 hours.
679 Supernatants were titrated on Vero E6 cells. The plaque assay was quantified 24 hours later.
680 Results are depicted as plaque forming units (PFU) per milliliter.

681

682 **Figure 4. B₂R antagonism exhibits a protective and suppressive effect on gene expression**
683 **profile of airway epithelial cells.**

684 GO term enrichment analysis, which results from the string network analysis of significant
685 DEGs from the gene expression analysis comparing infected NHBE pretreated with B₂R
686 antagonist with untreated infected NHBE (SARS-CoV-2 + B₂R antagonist *versus* SARS-CoV-
687 2). Depicted are enrichment of A) GO-term GO:0007186 “G protein-coupled receptor signaling
688 pathway” and B) GO-term GO:0006811 “Ion transport”. Genes that were significantly
689 upregulated in the comparison SARS-CoV-2 versus medium are highlighted in red. C) Venn
690 diagram showing the cut set of upregulated membrane-bound cell surface receptors in SARS-
691 CoV-2 *versus* medium and of downregulated DEGs in SARS-CoV-2 + icanbant *versus* SARS-

692 CoV-2 ($FC \geq 1.5$; $P \leq 0.05$). D) Heat map of gene expression analysis of the 35 membrane-bound
693 cell surface receptors defined in cut set from Fig.4C, all upregulated upon SARS-CoV-2
694 infection and downregulated upon pre-treatment with B₂R antagonist are depicted. Only entities
695 with significant changes between SARS-CoV-2 infection and medium (up) and between SARS-
696 CoV-2 + B₂R antagonist and SARS-CoV-2 (down) are shown (gene expression fold change
697 $FC \geq 1.5$ with $P < 0.05$). Color code indicates Log₂-fold change from low (blue) through 0 (white)
698 to high (red). Duplicate gene names indicate the abundance of two or more isoforms of the same
699 gene in the analysis.

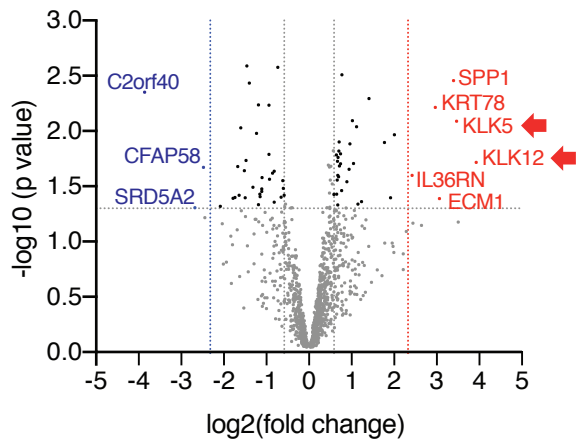
700
701

702 Table 1. Demographic data of patient cohort

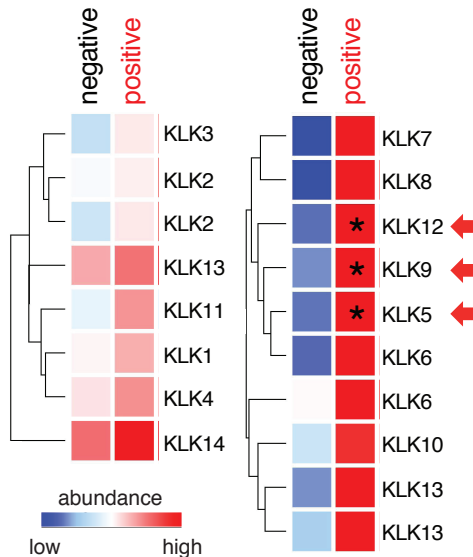
Parameter	Negative (n = 7)	Positive acute (n = 4)	p-value
Age (years)*	35.86 ± 3.86	37.50 ± 8.78	n.s.
Sex (m/f)	2/5	1/3	
IgM (ng/mL)	1.32 ± 0.28	4.34 ± 2.81	n.s.
IgG (ng/mL)	0.48 ± 0.08	67.08 ± 19.51	0.0061

703 negative: tested negative in SARS-CoV-2 qPCR; positive acute: tested positive in SARS-CoV-2 qPCR; IgM:
704 immunoglobulin M; IgG: immunoglobulin G; values are depicted as mean ± s.e.m.; n.s. not significant
705 *at informed consent procedure and inclusion into study

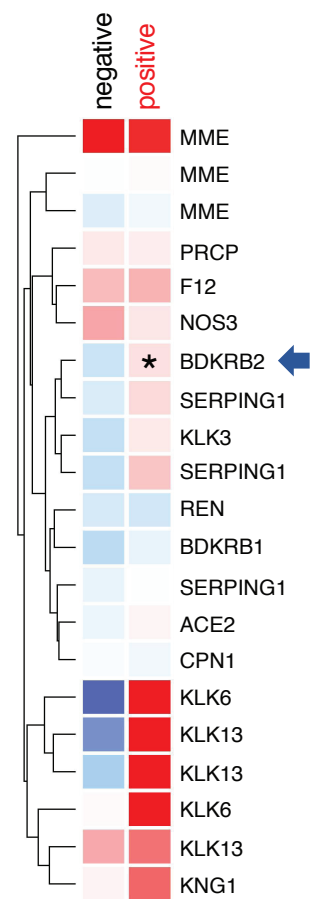
A - nasal transcriptome: secreted genes



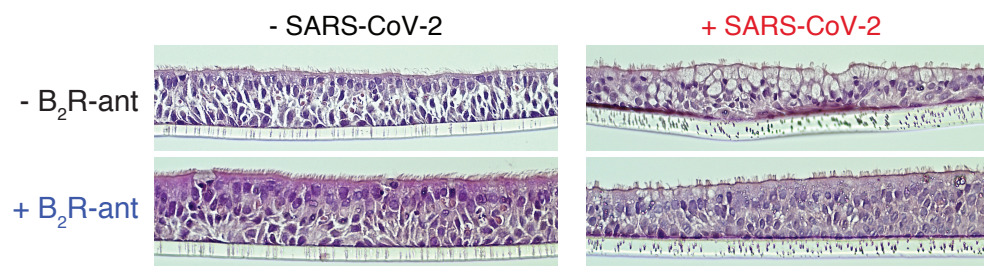
B - kallikreins



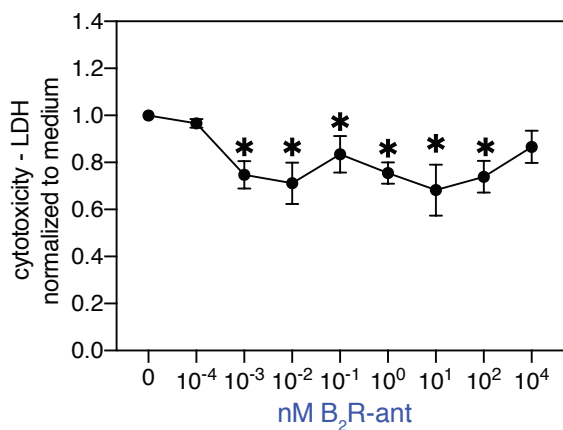
C - kinin-kallikrein system



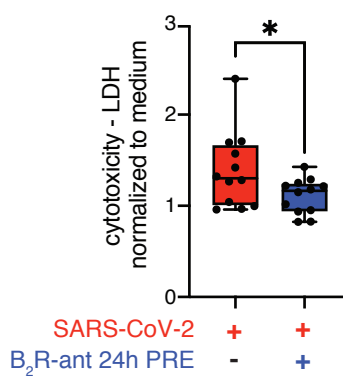
D - 3D bronchial organoid cultures



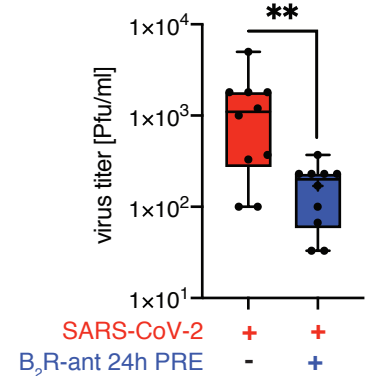
E - Cytotoxicity in uninfected NHBE



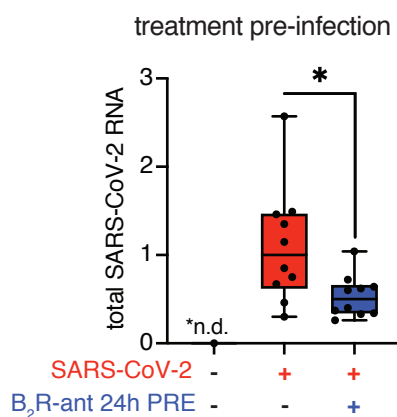
F - Cytotoxicity treatment pre-infection



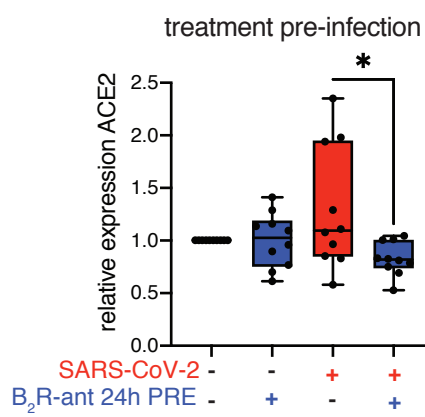
G - Plaque assay treatment pre-infection



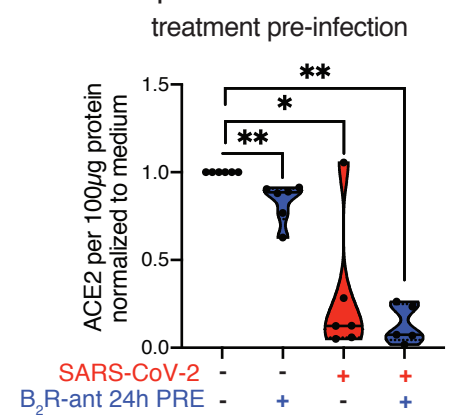
H - total viral RNA treatment pre-infection



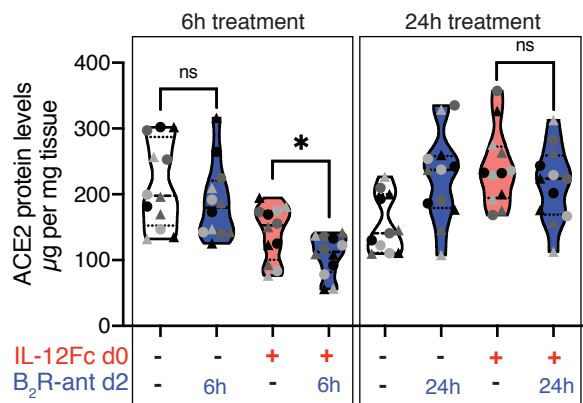
I - ACE2 mRNA levels treatment pre-infection



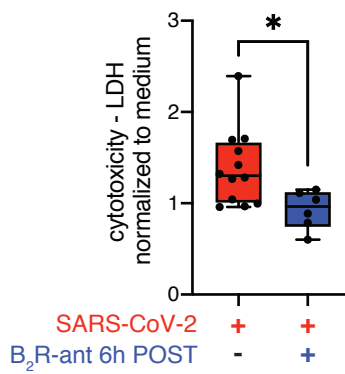
J - ACE2 protein levels treatment pre-infection



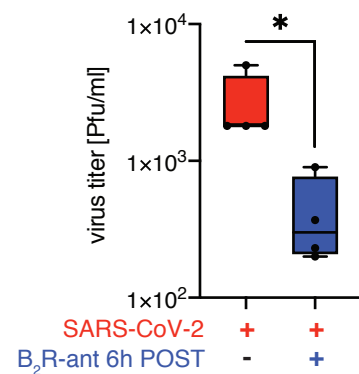
A - Mouse lung: ACE2 protein levels
treatment post airway inflammation



B - Cytotoxicity
treatment post-infection

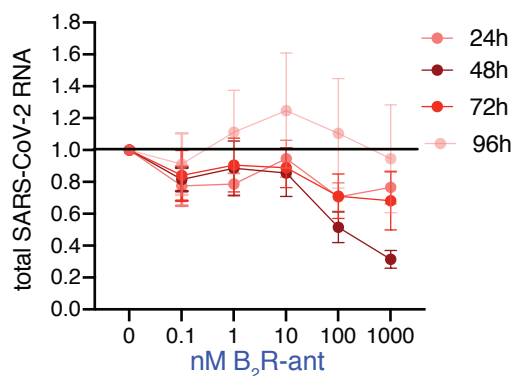


C - Plaque assay
treatment post-infection

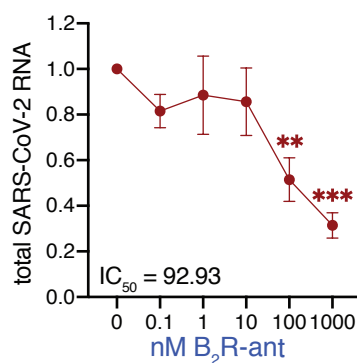


Treatment post-infection:

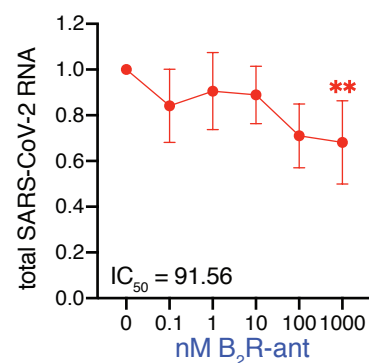
D - total viral RNA



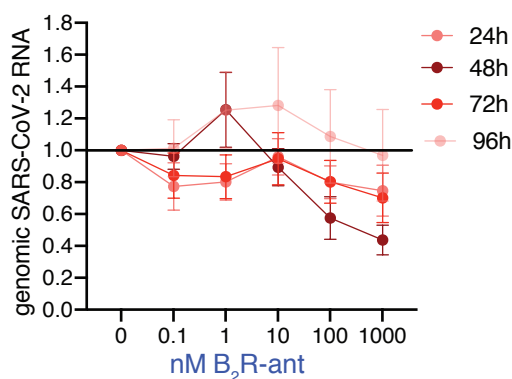
E - total viral RNA 48h



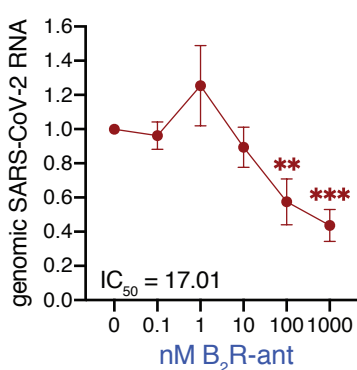
F - total viral RNA 72h



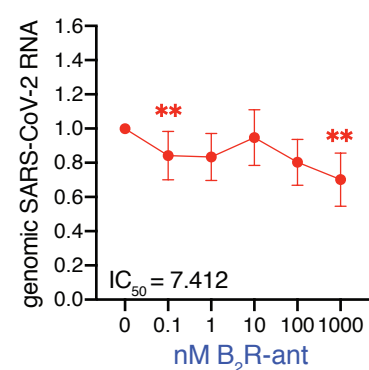
G - genomic viral RNA



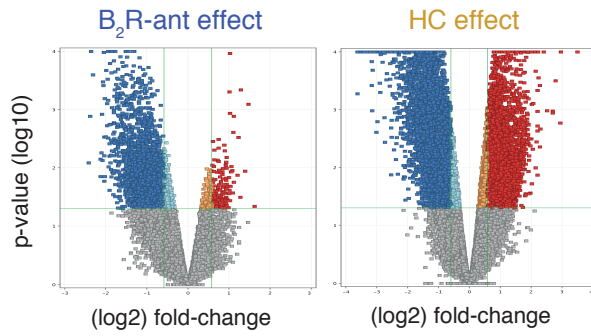
H - genomic viral RNA 48h



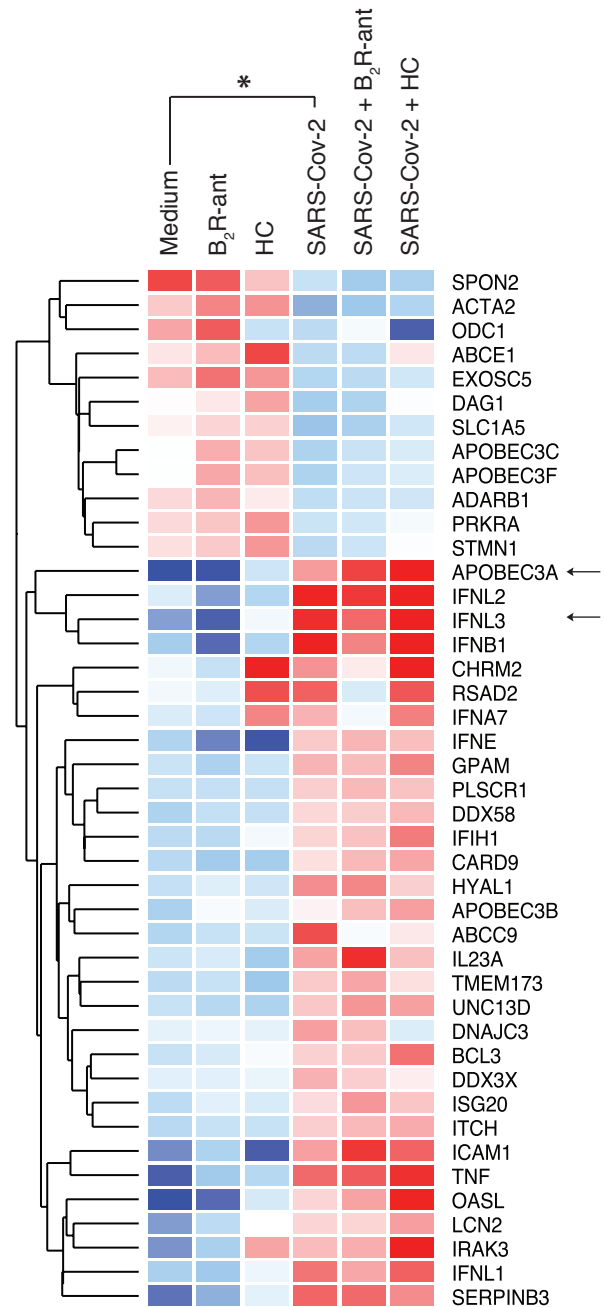
I - genomic viral RNA 72h



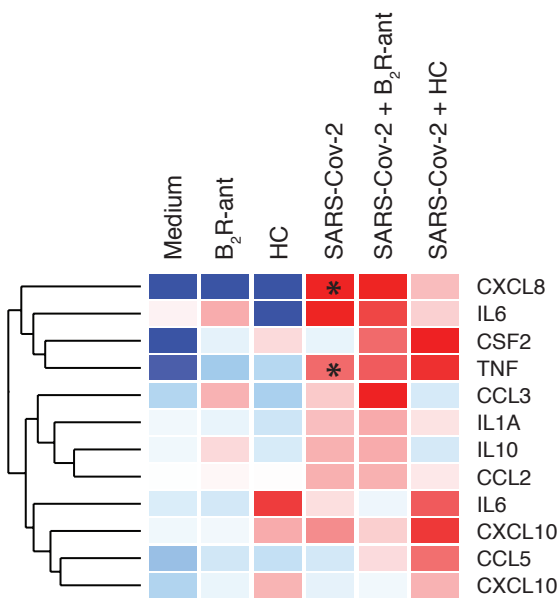
A - DEGs: B₂R-ant effect vs HC effect



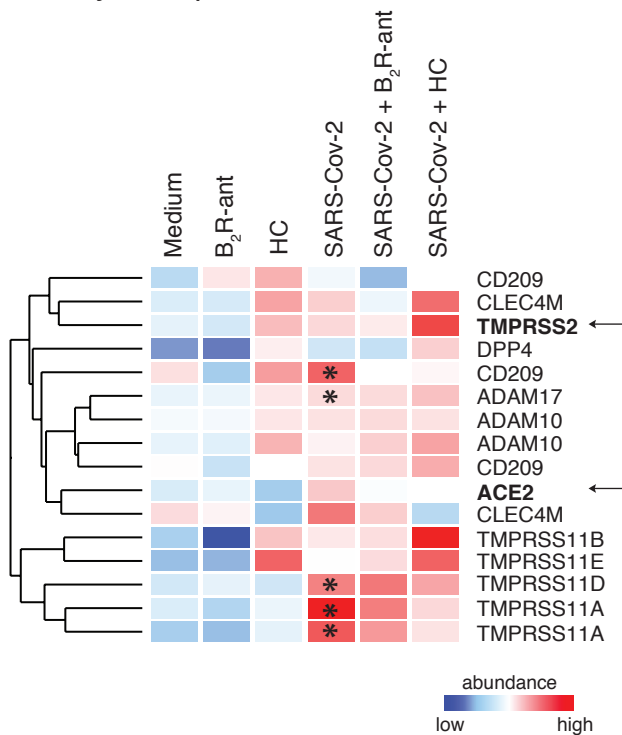
B - Antiviral response



C - Acute-phase response

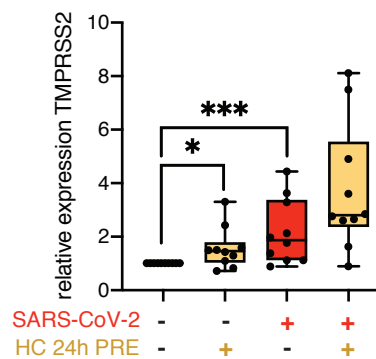


D - Entry Receptors



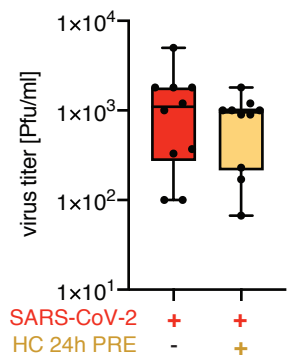
E - TMPRSS2 mRNA

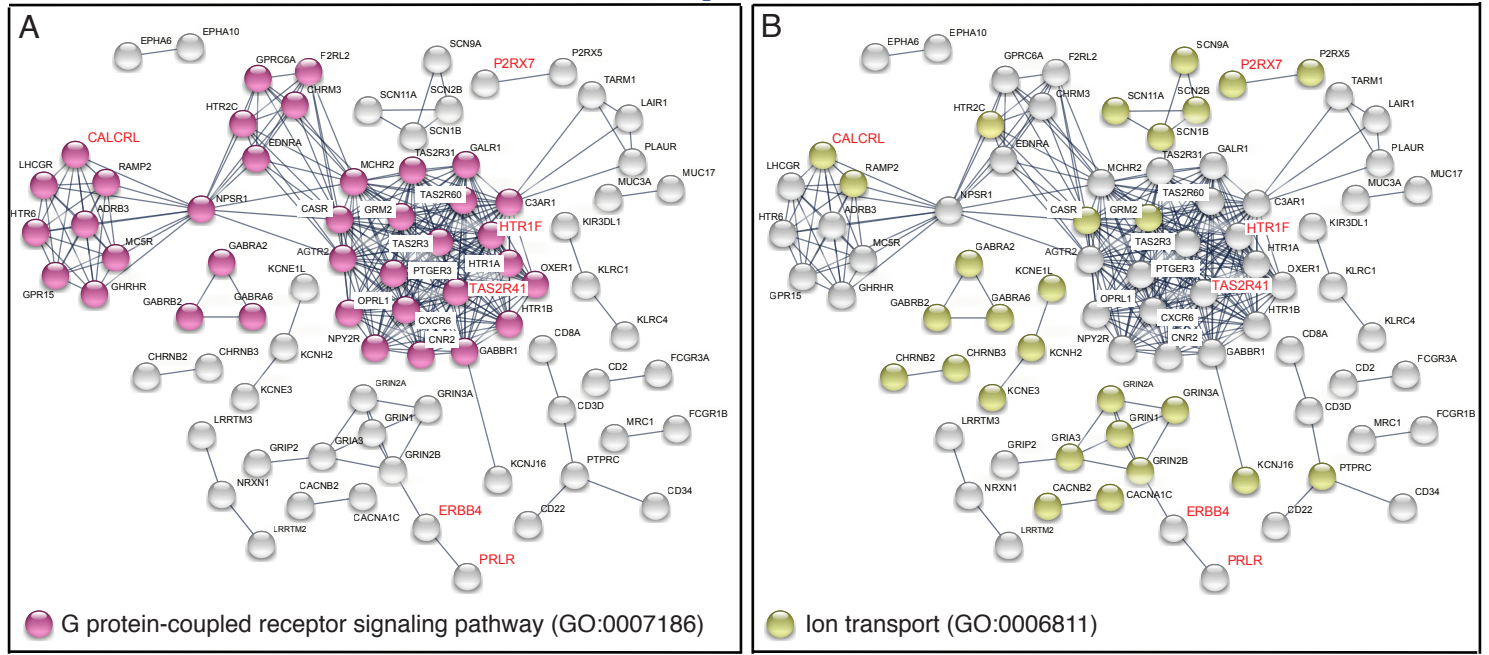
HC treatment pre-infection



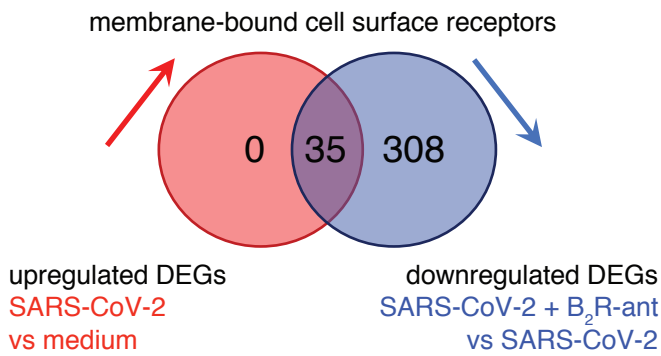
F - Plaque assay

HC treatment pre-infection





C - Counter-regulation of SARS-CoV-2-induced DEGs by B₂R antagonist



D - Membrane-bound cell surface receptors

